User-Centric Clustering in Cell-Free Networks with Dynamic TDD

Samuel S. Silva, Yuri C. B. Silva, Igor M. Guerreiro,
Victor F. Monteiro, Matheus D. Carneiro, and Abraão C. Albuquerque

***Abstract*— This work investigates the performance of a cell-free multiple-input multiple-output (MIMO) system with dynamic time division duplex (D-TDD), in which user-centric clustering algorithms are introduced as an additional stage to dynamically allocate access points (APs) at each time slot. This additional step enables an AP to simultaneously serve multiple user equipments (UEs) transmitting in the same direction. The implementation of these algorithms, incorporating an additional clustering step, is motivated by the fact that assigning an AP to serve multiple UEs does not significantly increase the system's interference levels; however, it can enhance the signal strength received from or by a given UE. The results indicate an advantage in applying an additional clustering step—or, conversely, a disadvantage in maintaining disjoint clusters of UEs transmitting in the same direction. This additional step yields greater performance improvements for uplink (UL) transmissions. This outcome can be explained by the fact that, when an AP is allocated to serve multiple UEs, the resulting increase in interference levels for downlink (DL) UEs is not substantial compared to the gain in received signal strength. In contrast, for UL transmissions, no additional interference is introduced, while the received signal strength increases significantly due to the larger number of antennas available to serve each UE.**

***Keywords*— Cell-free system, MIMO, D-TDD.**

I. Introduction

Wireless communication systems have been evolving to accommodate the increasing density of active UEs, provide higher data transmission rates and low latency and support intense data traffic [1]. In pursuit of these objectives, several studies have indicated that the cell-free network architecture, which combines a distributed deployment with advanced signal processing techniques, offers greater efficiency and scalability to meet these requirements [2]. A cell-free network is composed of a large number of APs distributed across the coverage area to provide more uniform and enhanced signal quality. These APs are connected to a central processing unit (CPU) via wired fronthaul links, which allow them to share information and perform joint transmissions to UEs [3], thereby improving signal reception and enhancing overall quality of service.

Samuel S. Silva, Yuri C. B. Silva, Igor M. Guerreiro, Victor F. Monteiro, Matheus D. Carneiro, and Abraão C. Albuquerque are with the Wireless Telecom Research Group (GTEL), Federal University of Ceará (UFC), Fortaleza, Brazil. E-mails {samuelserejo, yuri, igor, victor, matheus.carneiro, abraaoalbuquerque}@gtel.ufc.br. This work was supported in part by Brasil 6G project (01245.010604/2020-14, RNP and MCTI), in part by CNPq, in part by FUNCAP/Universal Grant UNI-0210-00043.01.00/23, in part by CAPES. The work of Victor F. Monteiro was supported by CNPq under Grant 308267/2022-2.

Nevertheless, despite the well-known advantages of this network architecture, most studies addressing scenarios with cell-free networks assume that the transmission direction allocation is performed statically, meaning that all APs in the system transmit simultaneously in the same mode and share the same frame configuration, which consists of a fixed division of time resources between UL and DL [4]. As a result of the growing heterogeneity of data traffic and rising demands for higher transmission rates, systems employing static time division duplex (TDD) tend to experience performance degradation and reduced capacity to support a large number of UEs, thereby requiring new strategies to address this limitation and to manage time resources more efficiently.

Given this set of factors, the implementation of dynamic TDD has emerged as a promising solution for managing the heterogeneous traffic demands and improving UE quality of service (QOS) through more efficient time resource utilization. The fundamental idea behind dynamic TDD is to configure the transmission frame of APs in a manner that best adapts to the system's instantaneous traffic demands. In traditional cellular scenarios with dynamic TDD, the frame configuration of each cell is typically adjusted individually, based solely on the traffic generated by UEs within that cell. However, in a cell-free scenario employing a user-centric approach, it is possible for a UE transmission frame to be configured in a more individualized manner, tailored to each users' specific traffic demands. This is made feasible through clustering techniques that allow each UE to be served by a disjoint cluster of APs exclusively dedicated to that UE, assuming a system in which the APs operate in half-duplex mode.

However, the implementation of dynamic TDD introduces new interference components due to the coexistence of UL and DL transmissions, such as inter-AP-interference (IAI) and inter-UE-interference (IUI). Given this issue, it has become clear that effective interference cancellation techniques are essential to enable the practical deployment of D-TDD. Some studies have addressed the cancellation of interference between access points by exploiting inter-AP communication over fronthaul links , a technique known as network-assisted full-duplex [5]. Other studies have explored the possibility of mitigating part of the UE-to-UE interference through a cluster-based grouping technique, while simultaneously considering the aforementioned IAI cancellation [6].

The main contribution of this work is the analysis of two clustering algorithms that perform an additional APs allocation step in a cell-free system with D-TDD. The motivation for implementing these algorithms is to enable APs to serve mul-

tiple UEs transmitting in the same direction, thereby increasing the number of antennas serving each UE and enhancing the experienced quality of service, without significantly increasing interference levels.

II. System Model

In this paper, we consider a cell-free MIMO system with D-TDD, consisting of L APs and K UEs, both randomly distributed over the coverage area and equipped with a single omnidirectional antenna. The APs are connected to a central CPU via fronthaul links and operate in half-duplex mode, meaning they can transmit only in one direction at a time. Fig. 1 illustrates the considered system.

A. Propagation model

This section describes the propagation channels existing in a cell-free MIMO system that operates in D-TDD. The propagation channel between the k-th transmitter and the l-th receiver, denoted by $h_{k,l} \in \mathbb{C}$, is modeled following a Rician distribution, having line of sight (LOS) and non line of sight (NLOS) components, and can be described as follows:

$$\mathrm{h}_{k,l} = \left[\sqrt{\frac{\bar{K}_{k,l}}{\bar{K}_{k,l}+1}} + \sqrt{\frac{1}{\bar{K}_{k,l}+1}} h_{k,l}^{(w)} \right] \beta_{k,l}\,, \tag{1}$$

where $h_{k,l}^{(w)} \sim \mathcal{CN}(0,1)$ is the NLOS component modeled following a Rayleigh uncorrelated distribution, $\beta_{k,l}$ represents the large scale coefficient, which models the path-loss and shadowing effects, and $\bar{K}_{k,l}$ is the Rician K-factor as in [7]. We can omit the steering vector in the equation, since each transmitter and receiver has only one antenna. The LOS probability is defined for each type of link. For example, the link between UEs and APs, as well as the link between two APs, is subject to LOS probability. For both types of link, the LOS probability can be defined as:

$$\begin{aligned} \mathrm{Prob}_{\mathrm{LOS}}(R) = 0.5 - \min\left(0.5,\, 5e^{-0.156/R}\right) \\ + \min\left(0.5,\, 5e^{-R/0.03}\right)\,, \end{aligned} \tag{2}$$

in which R is the distance between the transmitter and the receiver in km. Given the LOS probability, it is possible to determine the Rician K-factor K. If the channel is LOS, $K \sim \mathcal{N}(9,5)$ dB for both UE to AP or AP to AP links; if the channel is NLOS, then K is equal to zero according to [8]. We consider that the link between two UEs has no probability of being LOS.

The large-scale fading coefficient $\beta_{k,l}$ is defined as:

$$\beta_{k,l} = 10^{\frac{PL_{k,l}+\sigma_{sh}}{10}}\,, \tag{3}$$

where $\sigma_{sh} \sim \mathcal{N}\left(0,\sigma^2\right)$ and $PL_{k,l}$ represent the shadowing and path-loss gains in dB. The path-loss calculation varies according to the type of link being modeled and whether or not the channel is LOS. The calculation of path-loss for all link types and LOS conditions is implemented as in [9].

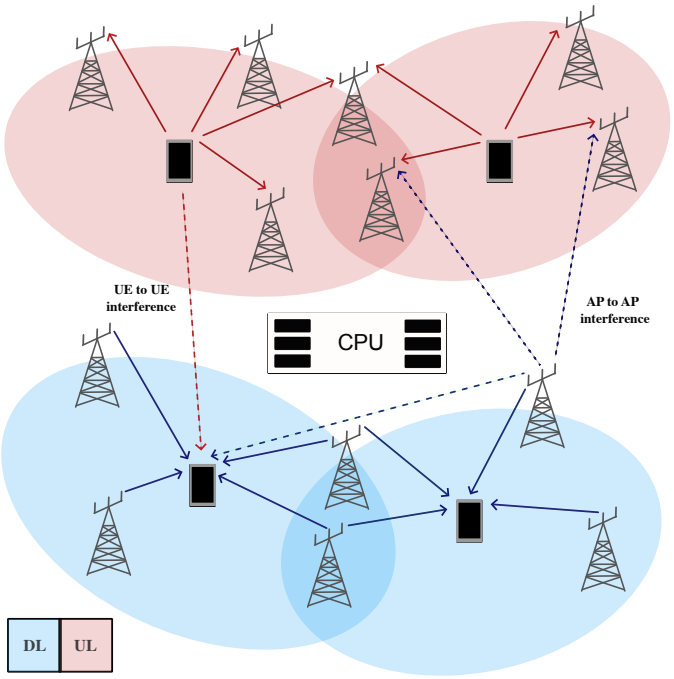

Fig. 1. Cell-Free system with dynamic time division duplex.

B. Signal model

In this section, we present the signal and spectral efficiency models for a cell-free system employing dynamic TDD for both UL and DL transmissions. As previously mentioned, the coexistence of transmissions in opposite directions gives rise to new types of interference, such as IAI and IUI. Moreover, the interference levels in the system vary continuously as traffic demands fluctuate, which necessitates the constant recalculation of spectral efficiency at each time slot.

We denote the channel vector between the k-th UE and the APs that compose the serving cluster C_k as $\mathbf{h}_{(C_k,k)} \in \mathbb{C}^{|C_k|\times 1}$, the channel vector between the interfering j-th UE and the AP cluster C_k as $\mathbf{h}_{(C_k,j)} \in \mathbb{C}^{|C_k|\times 1}$, the channel matrix between the AP clusters C_k and C_m as $\mathbf{H}_{(C_k,C_m)} \in \mathbb{C}^{|C_k|\times|C_m|}$ and the channel coefficient between the k-th UE and the j-th UE as $h_{k,j} \in \mathbb{C}$.

The received signal by AP cluster C_k operating in UL in the n-th slot is given by:

$$\begin{aligned} \mathbf{y}_k^{UL} = & \underbrace{\sqrt{\rho_{\mathrm{ul}}}\mathbf{h}_{(C_k,k)} x_k T_{\mathrm{ul}(k)}}_{\text{desired signal}} \\ & + \sum_{\substack{j=1 \\ j\neq k}}^{K} \underbrace{\sqrt{\rho_{\mathrm{ul}}}\mathbf{h}_{(C_k,j)} x_j T_{\mathrm{ul}(j)}(1-\delta_{(j)})}_{\text{UE-to-AP interference}} \\ & + \sum_{\substack{m=1 \\ m\neq k}}^{K} \underbrace{\mathbf{H}_{(C_k,C_m)}\mathbf{P}_{\mathrm{dl}(m)}\mathbf{w}_m s_m T_{\mathrm{dl}(m)}\delta_{(m)}}_{\text{AP-to-AP interference}} + \underbrace{\mathbf{z}_{\mathrm{ul}(k)}}_{\text{noise}}, \end{aligned} \tag{4}$$

where $\rho_{\mathrm{ul}} \in \mathbb{R}_+$ is the UL transmit power, $\mathbf{P}_{\mathrm{dl}(m)} \in \mathbb{R}_+^{|C_m|\times|C_m|}$ is a diagonal DL power allocation matrix relative to UE m, with each element in the diagonal indicating the square root of the power allocated to UE m at each AP of the AP cluster C_m, δ_k indicates the transmission direction of UE

k, with $\delta_k = 0$ indicating UL and $\delta_k = 1$ indicating DL; $T_{\text{ul}(k)}$ and $T_{\text{dl}(k)}$ denotes the presence or absence of data to transmit in the UL and DL queue of UE k; $\mathbf{w}_m \in \mathbb{C}^{|C_m|\times 1}$ denotes the transmit beamforming vector from cluster C_m for UE m and x_k and s_m denote the UL and DL unit power transmission symbols, respectively. The time indices of each component of the equation have been omitted so that they can be better visualized; however, it is extremely important to mention that some of these components vary over time. In a time slot, the amount of bits transmitted by the k-th UE operating in UL is given by:

$$R_k^{\text{ul}} = B\,\log_2\left(1 + \frac{\rho_{\text{ul}}\left|\mathbf{u}_k^T\mathbf{h}_{(C_k,k)}\right|^2 T_{\text{ul}(k)}}{\gamma_k^{UL}}\right) \times \tau_s, \quad (5)$$

where $\mathbf{u}_k \in \mathbb{C}^{|C_k|\times 1}$ represents the unit-norm receive beamforming vector for AP cluster C_k, τ_s is the slot duration, and γ_k^{UL} represents the sum of interference and noise components:

$$\gamma_k^{\text{UL}} = \sum_{\substack{j=1\\ j\neq k}}^{K} \rho_{\text{ul}}\left|\mathbf{u}_k^T\mathbf{h}_{(C_k,j)}\right|^2 T_{\text{ul}(j)}\left(1-\delta_{(j)}\right) + \sum_{\substack{m=1\\ m\neq k}}^{K}\left|\mathbf{u}_k^T\mathbf{H}_{(C_k,C_m)}\mathbf{P}_{\text{dl}(m)}\mathbf{w}_m\right|^2 T_{\text{dl}(m)}\delta_{(m)} + \sigma_{\text{ul}}^2. \quad (6)$$

The received signal by the k-th UE operating in DL in the n-th slot is given by:

$$y_k^{\text{DL}} = \underbrace{\mathbf{h}_{(C_k,k)}^T\mathbf{P}_{\text{dl}(k)}\mathbf{w}_k s_k T_{\text{dl}(k)}}_{\text{desired signal}} + \sum_{\substack{j=1\\ j\neq k}}^{K}\underbrace{\mathbf{h}_{(C_j,k)}^T\mathbf{P}_{\text{dl}(j)}\mathbf{w}_j s_j T_{\text{dl}(j)}\delta_{(j)}}_{\text{AP-to-UE interference}} + \sum_{\substack{m=1\\ m\neq k}}^{K}\underbrace{\sqrt{\rho_{\text{ul}}}\mathbf{h}_{m,k}x_m T_{\text{ul}(m)}\left(1-\delta_{(m)}\right)}_{\text{UE-to-UE interference}} + \underbrace{z_{\text{dl}(k)}}_{\text{noise}}. \quad (7)$$

In a time slot, the amount of bits transmitted for the k-th UE operating in DL is given by:

$$R_k^{\text{dl}} = B\,\log_2\left(1 + \frac{|\mathbf{h}_{(C_k,k)}^T\mathbf{P}_{\text{dl}(k)}\mathbf{w}_k|^2 T_{\text{dl}(k)}}{\gamma_k^{dl}}\right) \times \tau_s, \quad (8)$$

where γ_k^{dl} represents the sum of the interference and noise components perceived by the UE k:

$$\gamma_k^{\text{DL}} = \sum_{\substack{j=1\\ j\neq k}}^{K}|\mathbf{h}_{(C_j,k)}^T\mathbf{P}_{\text{dl}(j)}\mathbf{w}_j|^2 T_{\text{dl}(j)}\delta_{(j)} + \sum_{\substack{m=1\\ m\neq k}}^{K}\rho_{\text{ul}}|\mathbf{h}_{k,m}|^2 T_{\text{ul}(m)}\left(1-\delta_{(m)}\right) + \sigma_{\text{dl}}^2. \quad (9)$$

The cross link interference (CLI) terms are inexistent when all UEs are scheduled in the same transmission direction, whether UL or DL.

III. Frame Configuration

In this section, we describe how the frame is individually configured for each UE as in [6]. For this stage, the number of slots in a frame that will be reserved for UL transmissions is first calculated, as described next:

$$\tau_{\text{ul}(k)} = \text{round}\left\{\frac{Q_{\text{ul}(k)}}{Q_{\text{dl}(k)} + Q_{\text{ul}(k)}} \times N\right\}, \quad (10)$$

where round is a function that returns the nearest integer number, $Q_{\text{ul}(k)}$ and $Q_{\text{dl}(k)}$ denote the amount of uplink and downlink data, respectively, that are queued for UE k and N is the number of slots that compose a complete frame. After this, the frame for a given UE is configured as follows:

$$\delta_k[n] = \begin{cases} 0, & 1 \leq n \leq \tau_{\text{ul}(k)} \\ 1, & \tau_{\text{ul}(k)} < n \leq N \end{cases}. \quad (11)$$

IV. Clustering and grouping algorithms

In this work, we consider a primary clustering strategy, which consists of allocating a fixed and equal number of APs to each UE, ensuring that they are maintained in disjoint clusters, as in [6]. The motivation for this first step is to ensure that UEs can be served with a traffic configuration tailored to their specific needs. However, enforcing disjoint clusters requires defining a priority criterion for APs selection. In this initial allocation stage, AP selection is based on large scale fading: the UE with the highest total large-scale gain across all APs is given the highest priority and selects the APs for which it has the strongest gains. Moreover, it is important to highlight that this priority-based scheme may result in some UEs being assigned to APs with comparatively lower channel gains.

In order to enhance the system performance and introduce greater flexibility in AP allocation according to traffic direction, this work proposes the implementation of algorithms that allow APs transmitting in the same direction to serve multiple UEs as a complementary step to the baseline clustering strategy. Given the variability of transmission directions and traffic, this re-clustering step is performed recurrently in the system and becomes feasible in practice, as frame configurations of each UE are defined in advance, prior to transmission. This allows the CPU to compute the dynamic allocation AP allocation for the entire frame.

For this additional stage, two clustering algorithms originally designed for static time division duplex (S-TDD) cell-free networks were selected and executed separately for the group of UEs intending to transmit in the same mode. The two clustering algorithms share the use of the large-scale fading as a core selection metric, while also exhibiting individual variations in their design. Clustering based on large-scale fading effects takes into account the effects of path-loss and shadowing, but does not account for rapid variations in propagation channel, which allows a certain tolerance to variations in signal levels and greater flexibility in the allocation of network resources [10].

A. Dynamic Cooperation Clustering

This algorithm is characterized by the selection of the APs using the signal-to-noise-ratio (SNR) as the main criterion. The first step of this algorithm identifies the AP already assigned to the UE with the highest large-scale gain, which will be designated as the master AP [11]. Subsequently, a search is performed for APs that do not belong to the UE's current cluster, but satisfy the SNR condition. For the condition to be satisfied, the difference between the SNR of the candidate AP and that of the master AP, expressed in logarithmic scale, must be greater than or equal to a predefined threshold. The variation of this threshold can make the selection of APs more restrictive or more permissive.

B. Clustering Based on Large Scale Fading

In the fist stage of the algorithm, assuming that the CPU has knowledge of the large-scale fading effects for all possible links between the APs and UEs, the large-scale coefficients between all APs and UEs transmitting in the same mode are computed. Afterwards, all the gain values will be grouped in order to calculate a threshold factor α_{lsf} as follows:

$$\alpha_{lsf} = \frac{1}{K'}\frac{1}{L'}\sum_{k=1}^{K'}\sum_{l=1}^{L'}\beta_{k,l}, \tag{12}$$

in which K' denotes the number of UEs that intends to transmit in the same direction and L' denotes the amount of APs that are serving these UEs. If the large-scale coefficient between the k-th UE and the l-th AP $\beta_{k,l}$ is greater than, or equal to, α_{lsf}, the l-th AP will be allocated to serve it.

V. Simulation Results

The simulated cell-free scenario with D-TDD consists of $K = 30$ UEs and $L = 120$ APs distributed over a coverage area of 1200 square meters. Maximum ratio (MR) processing is considered for both transmit and receive beamforming vectors. We assume that all APs are connected to a central CPU via fronthaul links, which allows them to share information. Constant transmit power is assumed at each UE and at each AP. When applying the re-clustering step, in the case when an AP serves multiple UEs in the DL, the total AP power is divided equally among the streams of those UEs.

The system performance is evaluated using the cumulative distribution function (CDF) of the packet delay as the metric, with separate analyses for UL and DL performance. The packet traffic is modeled as a discrete-time queuing system, where packet arrivals follow a Poisson process, and both the queuing and dequeuing of packets are restricted to the beginning and end of each slot, respectively. We consider that the average inter-arrival time of packets varies according to packet type and UE traffic demand, being shorter for packets corresponding to the direction in which the UE has higher demand, and longer for those associated with the direction of lower demand. For UEs with symmetric traffic demand, the inter-arrival time is assumed equal for both directions. The packet delay is defined as the number of time slots it remains in the queue, counted from the moment it is enqueued until the moment it is dequeued. Simulation parameters listed system composition and packets traffic are listed in Table I.

TABLE I
Simulation Parameters

Parameter	Value
AP height	11.5 m
UE height	1.5 m
Bandwidth (B)	20 MHz
Uplink power	100 mW
Downlink power	1 W
Noise power Density	-174 dBm/Hz
Shadowing variance (σ^2_{sh})	4 dB
Slot duration	1 ms
DL packet size	50 kbytes
UL packet size	50 kbytes
Packet arrival interval	(UL, DL)
UL-heavy UE:	(8, 16) ms
DL-heavy UE:	(16, 8) ms
Symmetric UE:	(12, 12) ms

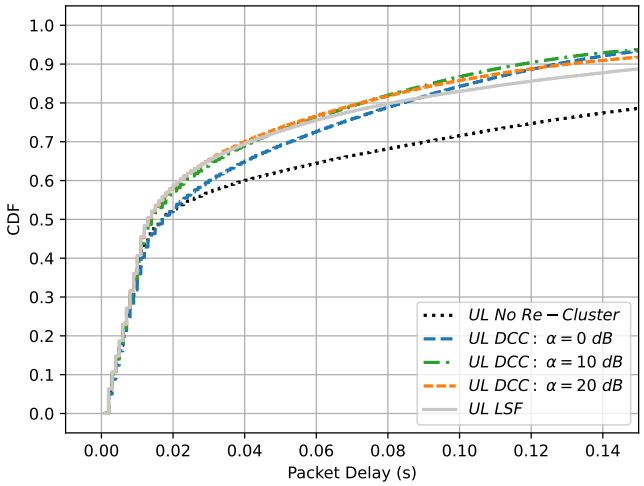

Fig. 2. Cumulative distribution function of uplink packet delay.

Figure 2 presents the results of the implemented clustering strategies in terms of the CDF of UL packet delay: the baseline clustering, the two additional algorithms, and the variations of one of them. From these results, it can be observed that the re-clustering strategies, based on the presented algorithms, reduced the UL packet delay. This outcome can be explained by the fact that the baseline clustering strategy, which enforces disjoint UE clusters, results in limited fairness in AP allocation. The additional clustering step partially mitigates this by allowing an AP to serve multiple UEs, thereby improving performance for UEs in disadvantaged conditions.

Among the implemented re-clustering strategies, the best performing methods were the DCC algorithm with a 20 dB threshold and the large-scale-based approach, yielding 56.04% and 53.85% reductions in packet delay at the 70th percentile, respectively, relative to the baseline clustering. For the same percentile value, the DCC algorithm with thresholds of 0 and 10 dB achieved reductions of 41.76% and 53.85% in packet delay compared to the fully disjoint scenario.

At the 90-th percentile, the DCC algorithms with thresholds of 20 dB and 10 dB achieved packet delay reductions of 61.99% and 65.50%, respectively, while the large-scale-based method resulted in a 51.75% reduction. These results reveal a small performance gap between the algorithms at this percentile level, being more significant between the DCC algorithms and the large-scale-based method and less significant between the DCC with different thresholds.

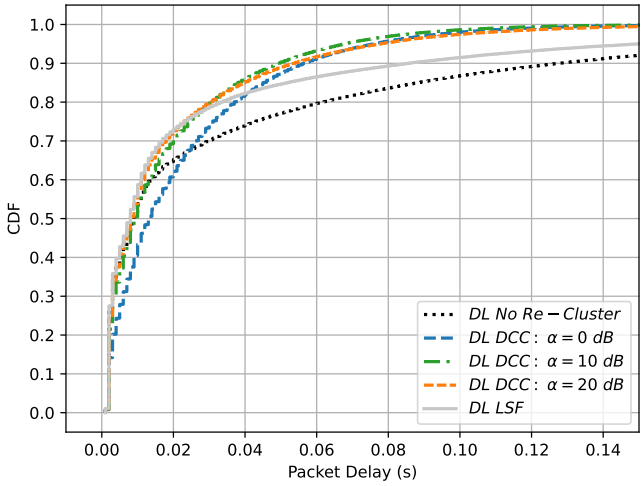

Fig. 3. Cumulative distribution function of downlink packet delay.

Figure 3 presents the CDF of DL packet delay for the considered clustering strategies. From these results, it can be observed that re-clustering strategies also led to performance gains. However, the packet delay reductions were considerably smaller than those observed in the UL. This outcome can be explained by the fact that, when serving multiple UEs, the transmission power of an AP is divided among the symbols to be transmitted. This leads to a reduction in the signal strength of interest for each UE and an increase in interference levels due to the symbols of other UEs.

For the DL case, among the implemented algorithms, the DCC with a 20 dB threshold and the large-scale-based method once again achieved the best results at the 70-th percentile, showing reductions of 40.0% and 43.33%, respectively, in DL packet delay compared to the disjoint cluster scenario. For the same percentile value, the DCC algorithm with thresholds of 0 and 10 dB resulted in reductions of 13.33% and 33.33% in delay at this percentile. At the 90-th percentile, the DCC algorithms with thresholds of 20 dB and 10 dB achieved packet delay reductions of 57.81% and 60.94%, respectively, while the large-scale-based method resulted in a 32.81% reduction compared to the disjoint cluster scenario.

VI. Conclusion

In this work, we evaluate the performance of a cell-free MIMO system with D-TDD under different additional re-clustering strategies, while considering distinct propagation conditions for each type of link in the system. The system initially adopts a baseline clustering method that enforces disjoint UEs clusters.

Based on the obtained results, we conclude that implementing the re-clustering step improves system performance in terms of packet delay, compared to fully disjoint AP clusters. However, depending on the threshold value, the DCC algorithm may degrade system performance due to the fact that the gain of having an additional AP may not compensate for the additional interference. For the packet delays on the UL, the DCC algorithm with thresholds of 10 and 20 dB and the large-scale based algorithm obtained satisfactory results and showed a reduction in packet delay compared to the disjoint clusters scenario.

Among the algorithms that were implemented, the DCC with threshold of 20 dB and 10 dB and the large-scale based algorithm obtained the most satisfactory results and outperformed the disjoint clusters scenario. On the other hand, the DCC with 0 dB threshold, which becomes more permissive for the selection of APs, obtained results that were not as satisfactory or even worse compared to the disjoint scenario. This result arises because disjoint clustering may force UEs to connect to APs with weak large-scale channel gains. The implementation of the re-clustering step helps mitigate this issue by allowing APs to be shared among UEs, enabling those in unfavorable conditions to be served by APs offering stronger large-scale gains.

References

[1] A. Chowdhury and C. R. Murthy, "Half-duplex APs with dynamic TDD versus full-duplex APs in Cell-Free systems," *IEEE Transactions on Communications*, vol. 72, no. 7, pp. 3856–3872, 2024.

[2] S. Chen, J. Zhang, J. Zhang, E. Björnson, and B. Ai, "A survey on user-centric cell-free massive MIMO systems," *Digital Communications and Networks*, vol. 8, no. 5, pp. 695–719, 2022, ISSN: 2352-8648.

[3] Ö. T. Demir, E. Björnson, and L. Sanguinetti, "Foundations of user-centric cell-free massive MIMO," *Foundations and Trends® in Signal Processing*, vol. 14, no. 3–4, pp. 162–472, 2021, ISSN: 1932-8354.

[4] M. Andersson, T. T. Vu, P. Frenger, and E. G. Larsson, "Joint optimization of switching point and power control in dynamic TDD cell-free massive mimo," in *Proc. 57th Asilomar Conference on Signals, Systems, and Computers*, IEEE, Oct. 2023, pp. 988–992.

[5] D. Wang, M. Wang, P. Zhu, J. Li, J. Wang, and X. You, "Performance of network-assisted full-duplex for cell-free massive MIMO," *IEEE Transactions on Communications*, vol. 68, no. 3, pp. 1464–1478, 2020.

[6] H. Kim, H. Lee, T. Kim, and D. Hong, "Cell-free mMIMO systems with dynamic TDD," in *Proc. IEEE 95th Vehicular Technology Conference (VTC2022-Spring)*, 2022, pp. 1–6.

[7] C. D'Andrea, A. Garcia-Rodriguez, G. Geraci, L. G. Giordano, and S. Buzzi, "Analysis of UAV communications in cell-free massive MIMO systems," *IEEE Open Journal of the Communications Society*, vol. 1, pp. 133–147, 2020.

[8] 3GPP, "Study on channel model for frequencies from 0.5 to 100 ghz," 3rd Generation Partnership Project (3GPP), Technical Report TR 38.901, version v17.0.0, Mar. 2022, Online. Available: `https://www.3gpp.org/ftp/Specs/html-info/38901.htm`.

[9] F. R. V. Guimarães, G. Fodor, W. C. Freitas, and Y. C. B. Silva, "Pricing-based distributed beamforming for dynamic time division duplexing systems," *IEEE Transactions on Vehicular Technology*, vol. 67, no. 4, pp. 3145–3157, 2018.

[10] S. Mashdour, S. Salehi, R. C. de Lamare, A. Schmeink, and J. P. S. H. Lima, "Clustering and scheduling with fairness based on information rates for cell-free MIMO networks," *IEEE Wireless Communications Letters*, vol. 13, no. 7, pp. 1798–1802, 2024.

[11] E. Björnson and L. Sanguinetti, "Scalable cell-free massive MIMO systems," *IEEE Transactions on Communications*, vol. 68, no. 7, pp. 4247–4261, 2020.